

N O T I C E

THIS DOCUMENT HAS BEEN REPRODUCED FROM
MICROFICHE. ALTHOUGH IT IS RECOGNIZED THAT
CERTAIN PORTIONS ARE ILLEGIBLE, IT IS BEING RELEASED
IN THE INTEREST OF MAKING AVAILABLE AS MUCH
INFORMATION AS POSSIBLE

RESEARCH OF THE STATE OF CONVECTION
IN THE EARTH'S MANTLE

Grant NCC 5-10

Final Report

For the period 1 May 1979 through 28 February 1981

(NASA-CR-163989) RESEARCH OF THE STATE OF
CONVECTION IN THE EARTH'S MANTLE Final
Report, 1 May 1979 - 28 Feb. 1981
(Smithsonian Astrophysical Observatory)
27 p HC A03/MF A01

N81-20639

CSCL J8G G3/46 41718

Unclassified

Principal Investigator
Dr. Micheline C. Roufosse

Prepared for
National Aeronautics and Space Administration
Goddard Space Flight Center
Greenbelt, Maryland 20771

March 1981

Smithsonian Institution
Astrophysical Observatory
Cambridge, Massachusetts 02138

The Smithsonian Astrophysical Observatory
and the Harvard College Observatory
are members of the
Center for Astrophysics



RESEARCH OF THE STATE OF CONVECTION
IN THE EARTH'S MANTLE

Grant NCC 5-10

Final Report

For the period 1 May 1979 through 28 February 1981

Principal Investigator

Dr. Micheline C. Roufosse

Prepared for
National Aeronautics and Space Administration
Goddard Space Flight Center
Greenbelt, Maryland 20771

March 1981

Smithsonian Institution
Astrophysical Observatory
Cambridge, Massachusetts 02138

The Smithsonian Astrophysical Observatory
and the Harvard College Observatory
are members of the
Center for Astrophysics

TABLE OF CONTENTS

	<u>Page</u>
I Introduction	1
II Method	2
III Results	2
A Study of the Walvis Ridge and Rio Grande Rise	2
B Study of Several Seamount Chains in the Pacific Ocean	11
C Study of the North Atlantic Ocean	20
IV Conclusion	23

I Introduction

Under this research grant, we studied studied the behavior and mechanical properties of the lithosphere. This is a prerequisite to an understanding of the mechanisms and processes that occur in the earth's mantle, which are masked by the lithosphere. For this study, we used geoid heights derived from the GEOS-3 and SEASAT radar altimeters. The study of the correlation between bathymetry and geoid heights gives information on the mechanical properties of the lithosphere, such as its thickness, which is related to the age of the lithospheric plate. By probing several locations spanning varied temporal situations, we are able to retrace the time evolution of the lithospheric plates.

We also believe that a systematic study of this type will lead to one of the following predictive capabilities: location of unknown seamounts from the knowledge of the geoid heights, prediction of gravity field from the knowledge of the topography and past history of the relief, or insight into the history of a region from the knowledge of both topography and geoid heights. To achieve this aim, several seamount chains, islands, and ridges must be investigated. Several geographical areas have already been studied, including the Walvis Ridge and Rio Grande Rise in the Southern Atlantic Ocean and several seamount chains in the Central Pacific Ocean. Conclusion of the present study indicate that two main factors influence geoid height: conditions of creation and age of the lithosphere at the time of loading.

II Method

In this project, we restricted ourselves to the study of linear bathymetric features, i. e., seamount chains. In studying such features, it is legitimate to consider individual satellite passes crossing the chain of seamounts at an angle as close as possible to 90 degrees. It is therefore unnecessary to go through the tedious procedure of adjusting all satellite passes into a coherent network by calculating and removing a bias and trend. Furthermore, dealing with individual satellite passes is ideal for studying the evolution along a seamount chain.

To account for the geoid signals observed so far, two models were developed: the thin-elastic-plate model and the Airy model (see, for example, McKenzie and Bowin, 1976). The thin-elastic-plate model applies when a load has been developed on a thin plate of finite thickness which is subsequently deformed. The magnitude and wavelength of the deformed area depend mostly on the flexural rigidity, which is itself proportional to the cube of the lithospheric thickness. The Airy-type model applies when the load was created simultaneously with the lithosphere (or on zero thickness lithosphere) and developed light roots in order to establish local or regional isostatic equilibrium. The methodology has been described in Roufosse (1979) and will be summarized here.

The first step in our procedure is to calculate theoretical filters in wavenumber space using variable parameters for both models (for example, see Figure 1). We then Fourier-transformed these functions in normal space. Next, the bathymetry was reconstructed as rigorously as possible along the subsatellite position using available contour charts (the Uchupi charts were used in the Atlantic Ocean). Lastly, the filters were convolved with the bathymetry in order to produce a set of theoretical geoid profiles to be compared with the observed geoid heights.

III Results

A. Study of the Walvis Ridge and Rio Grande Rise

The Walvis Ridge is aseismic and is made up of three main segments:

1) An eastern segment, extending continuously from the African margin to longitude 6 degrees E and trending east-northeast to west-southwest. It is approximately 600 km long and 100 to 200 km wide.

2) A central segment, trending north-south. This segment is lower and narrower than the eastern segment and is approximately 500 km long.

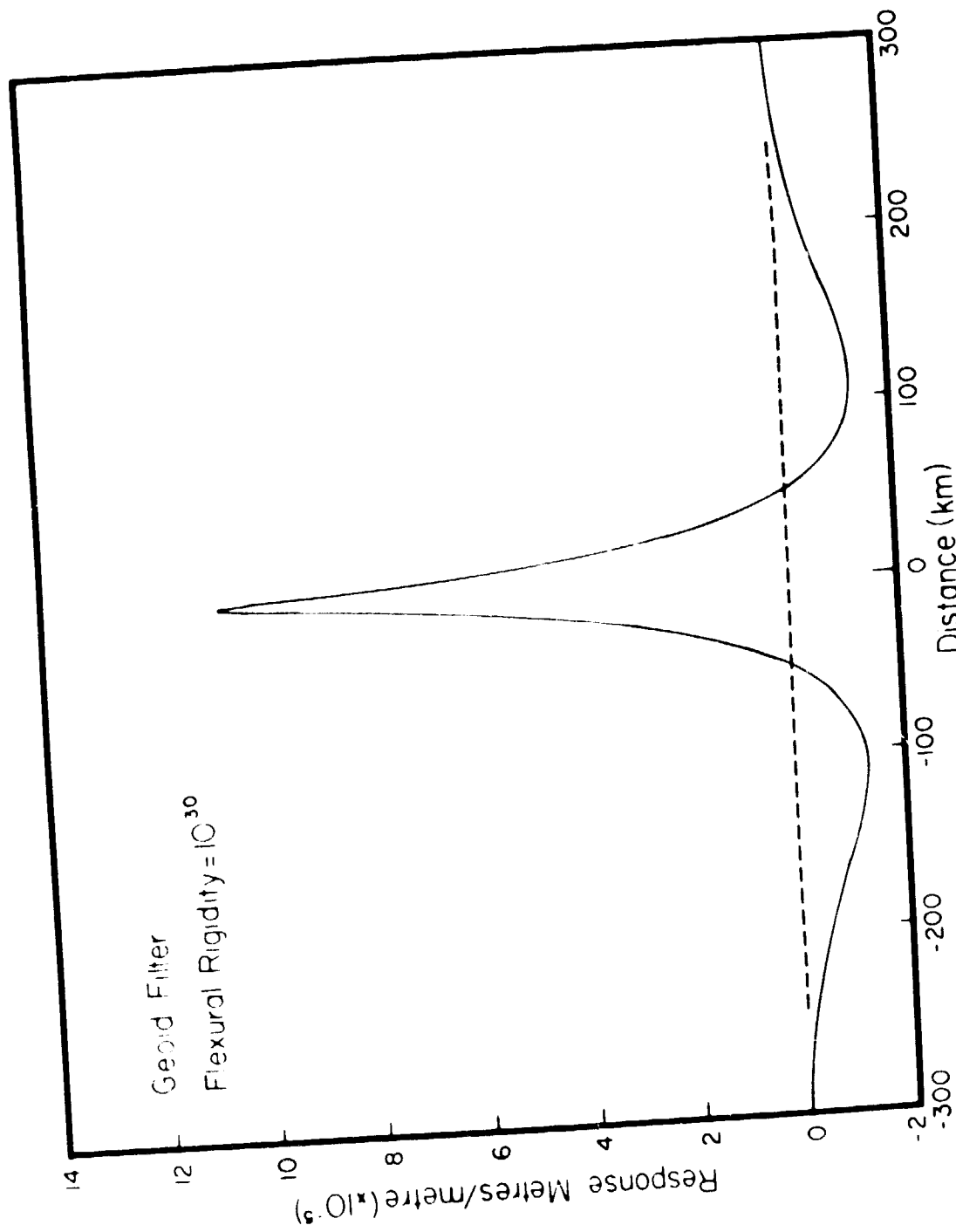


Figure 1. Geoid filter calculated by using a thin-elastic-plate model and a flexural-rigidity value of 10^{30} dyne-cm.

3) A western segment, made up of individual seamounts and divided into two branches, a sharp and elevated branch and a less marked northern branch. It extends to the Mid-Atlantic Ridge in the vicinity of Tristan da Cunha and Gough Islands.

There are two main hypothesis concerning the origin of the Walvis Ridge. The first is that it formed synchronously with the opening of the South Atlantic and resulted from hot spots (Morgan, 1971, 1972a, b; Le Pichon and Hayes, 1971; Francheteau and Le Pichon, 1972). The second is that it was created after the opening of the South Atlantic and is related to a major uplift (Ewing, Le Pichon, and Ewing, 1966; Maxwell and others, 1970). To distinguish between these two hypotheses, several investigators (Goslin, Mascle, Sibuet, and Hoskins, 1974; Goslin and Sibuet, 1975; Dingle and Simpson, 1976) have made use of all the information available for the eastern section of the ridge: bathymetry, seismic profiles, magnetic anomalies, age of the load, sedimentary distribution, morphology and constitution of the ridge, and gravity data. They all concluded that the easternmost section of the ridge was formed simultaneously with the lithosphere, on the ridge, by a mantle hot spot. Further, it is probably controlled by lines of weakness in the lithosphere such as tranforms faults. By no means can it represent a load superimposed on the lithosphere; this is ruled out by the gravity anomalies that suggest compensating roots down to a depth of about 25 km.

If we observe the direction of the Walvis Ridge, it is incompatible with a fixed hot-spot origin. It has been postulated that after the eastern segment was formed, approximately 127 to 80 m.y.b.p., the South Atlantic opening pole shifted at about 80 m.y.b.p. (Le Pichon and Hayes, 1971). It is likely that the center of the volcanic activity, which was responsible for creating the central section of the Walvis Ridge, moved southward at that time. The hot spot then presumably moved to the location of Tristan da Cunha, where it created the western section of the ridge, which thus developed on older lithosphere. If that is true, a thin-elastic-plate model, similar to that used for the Hawaiian and Marshall-Gilbert Islands (Roufosse, 1979) should be best suited to describe the western section of the Walvis Ridge. We used geoid heights derived from the GEOS-3 radar altimeter to investigate the structure of the Walvis Ridge and selected 16 satellite passes evenly spaced along the whole length of the ridge, as seen in Figure 2. We applied the Airy model with variable plate thickness and the thin-elastic-plate model with variable flexural rigidity to all these profiles. Eight of the profiles are presented in Figures 3 and 4. The eastern section of the ridge shows strong broad and asymmetrical signals with occasional dual structures, which account for the two separate ridges forming that section: the Valdivia Bank and the Frio Ridge. The central section reveals weaker and narrower signals, while the western section shows dual signals, a sharp

and intense southern peak and a weak northern signal. The geoid heights thus faithfully reflect the bathymetry of the area.

In the eastern section of the Walvis Ridge, the thin-elastic-plate value for the flexural rigidity that best accounts for the intensity of the observed geoid is very large, of the order of 2.5×10^{30} dyne-cm. This model, however, gives negative aisles that are not apparent in the observed geoid; moreover, the width of the theoretical signal is too large. Therefore, we tried the Airy model, which, in most of the passes observed, best reproduced the observed geoid for a local lithospheric thickness T of 25 km, as seen in Figures 5 and 6. This thickness, however, is larger than the average thickness along the whole profile. The Airy crustal thickening T can be defined by

$$T = \frac{h}{2} + \frac{t}{2} + T_c,$$

where h is the height of the ridge above the sea floor and t is the depth of the root below the bottom of the lithosphere. The Airy crustal thickness determined in that region is thus of the order of 20 km. We believe that the Airy model constitutes a much better description of the area; further, it fits with other available data, such as the age of the lithosphere, the age of the load, gravity data, and theories concerning the opening of the South Atlantic.

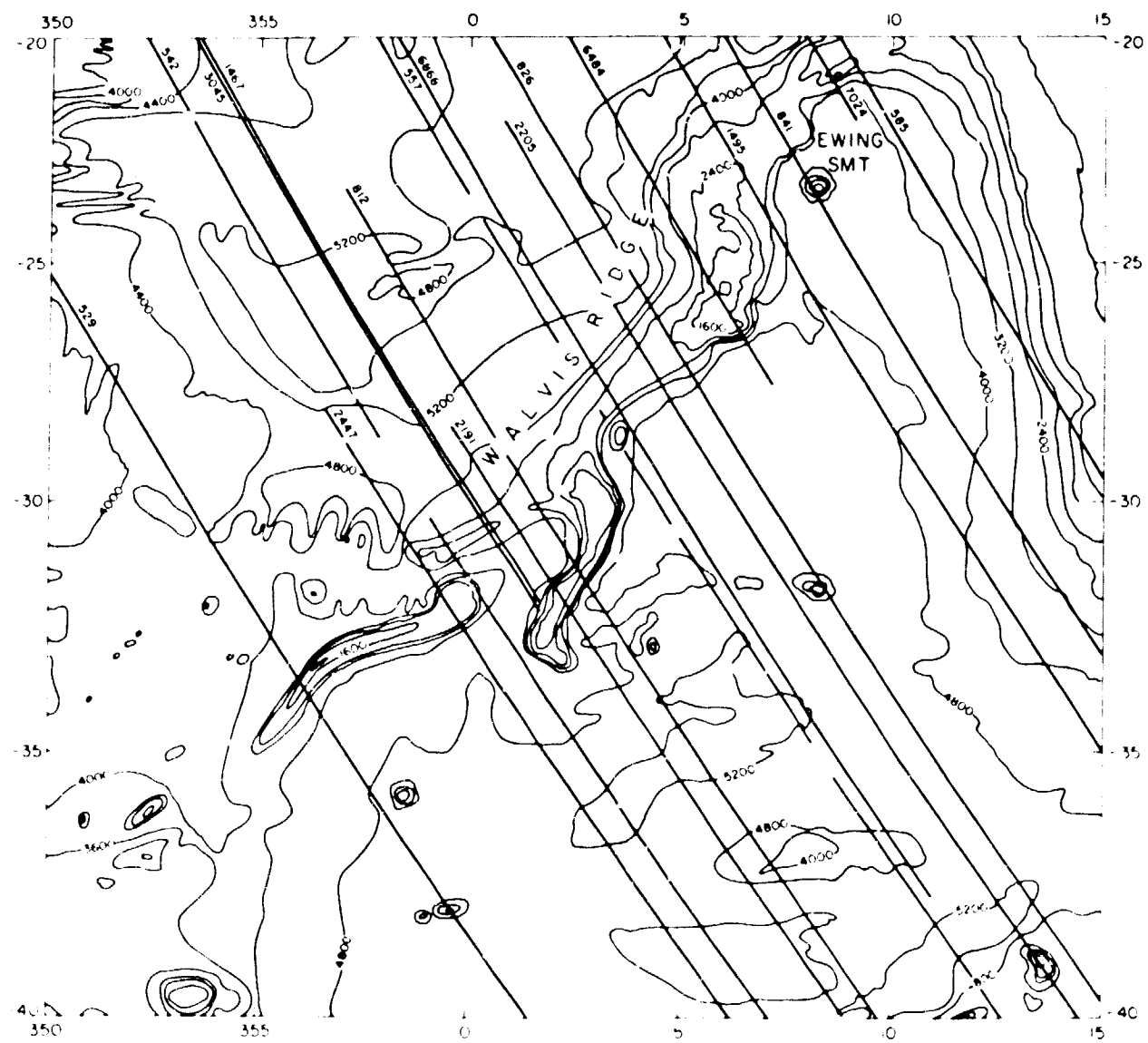


Figure 2. Bathymetry of the Walvis Ridge area and plot of the satellite passes selected over that region.

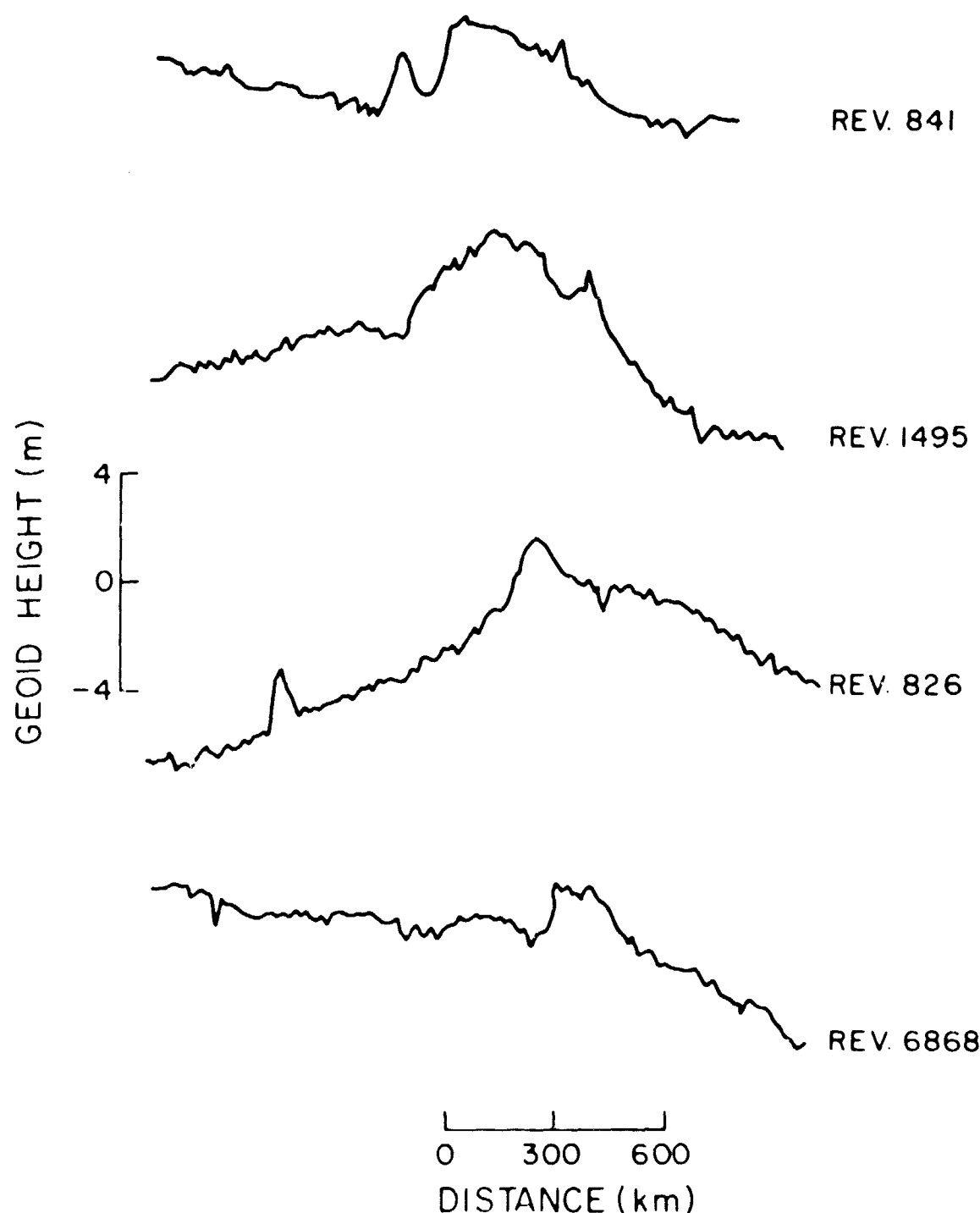


Figure 3. Four observed geoid profiles over the eastern and central sections of the Walvis Ridge, represented with respect to a reference geoid of degree and order 16.

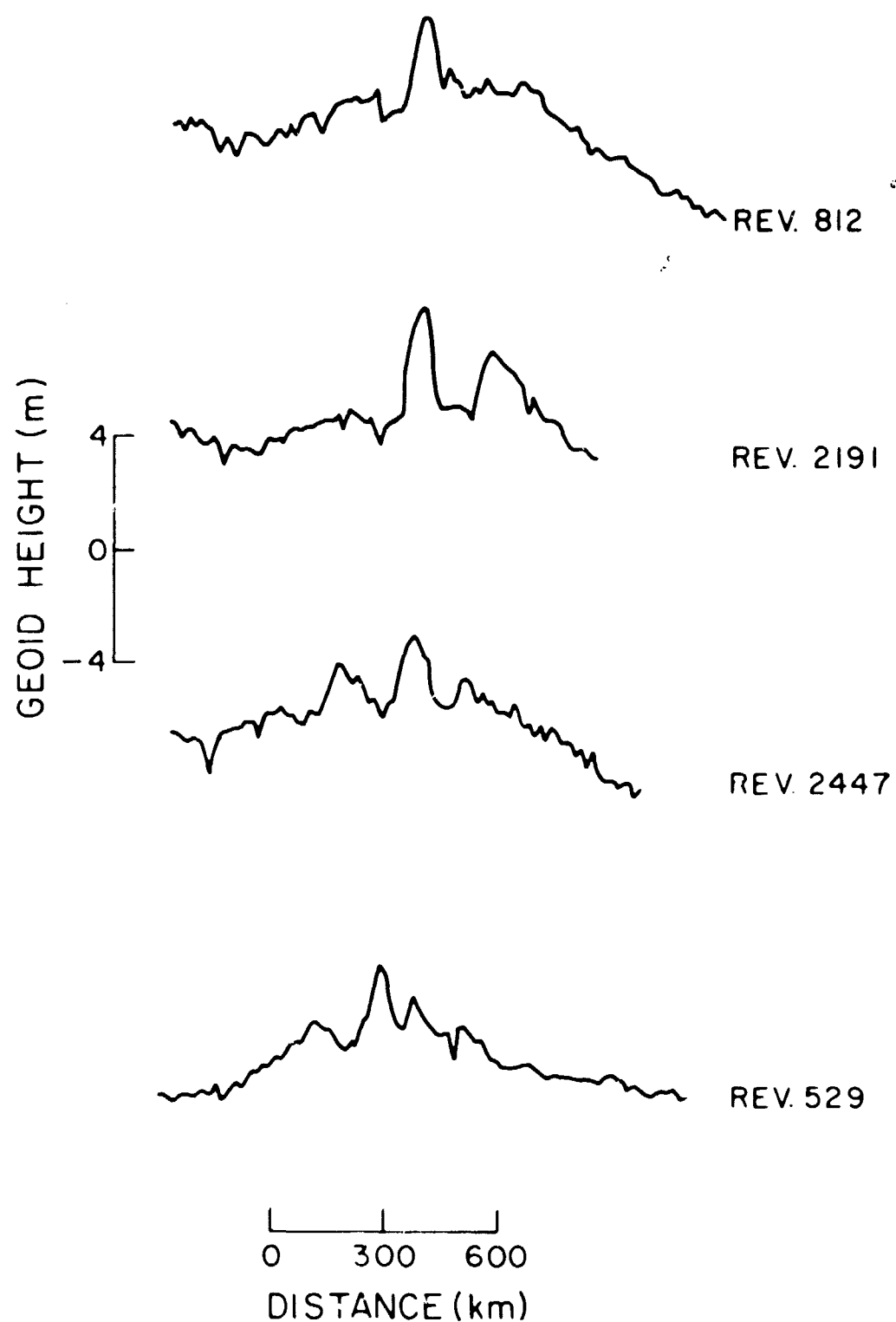


Figure 4. Four observed geoid profiles over the western section of the Walvis Ridge, represented with respect to a reference geoid of degree and order 16.

REV. 585

T = 25

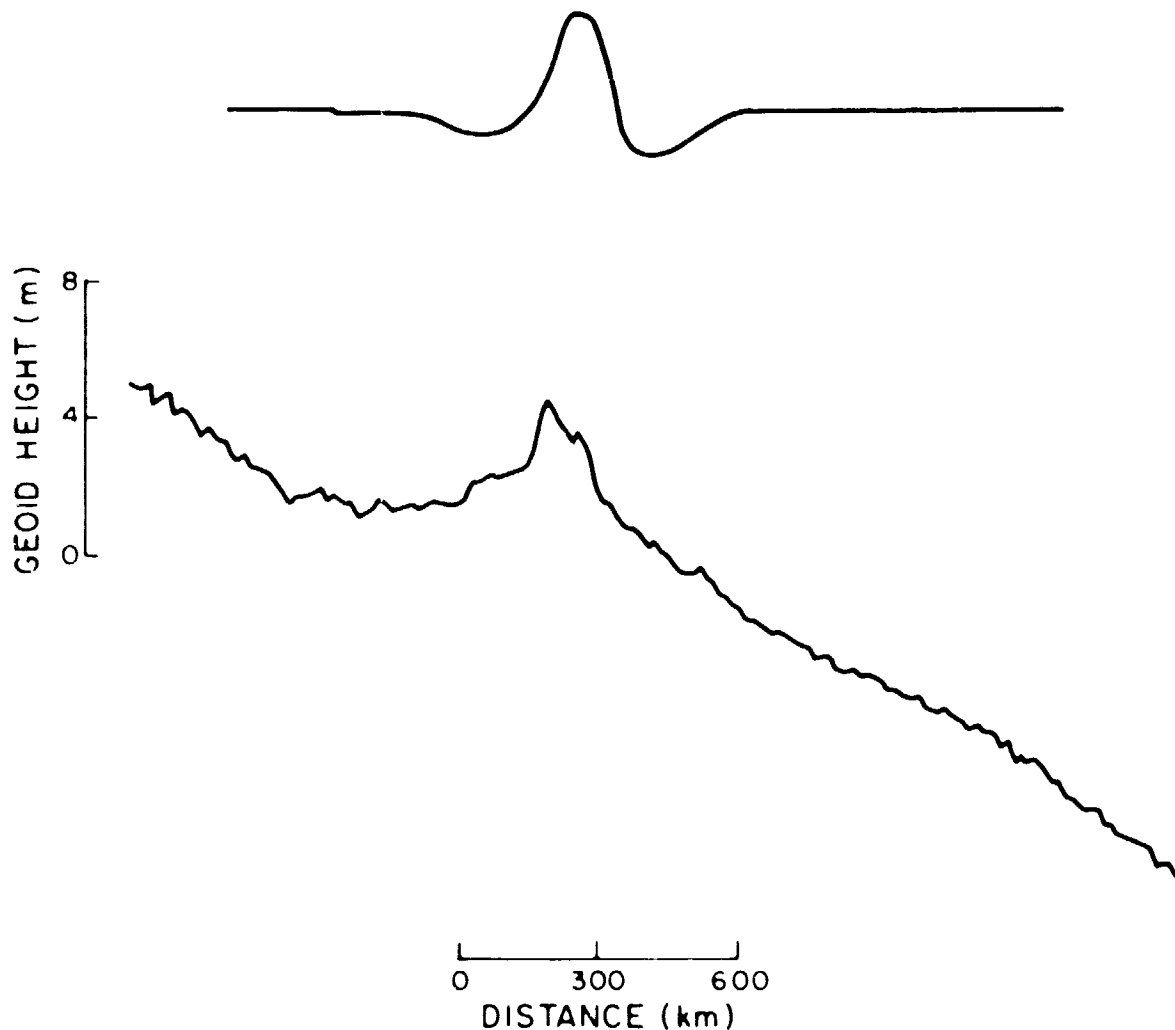


Figure 5. Predicted (top) and observed (bottom) geoid height for satellite revolution number 585 over Walvis Ridge. The top profile uses the Airy-type model with a crustal thickness of 25 km. The observed geoid is given with respect to a reference geoid of degree and order 16.

REV. 7024

T=25

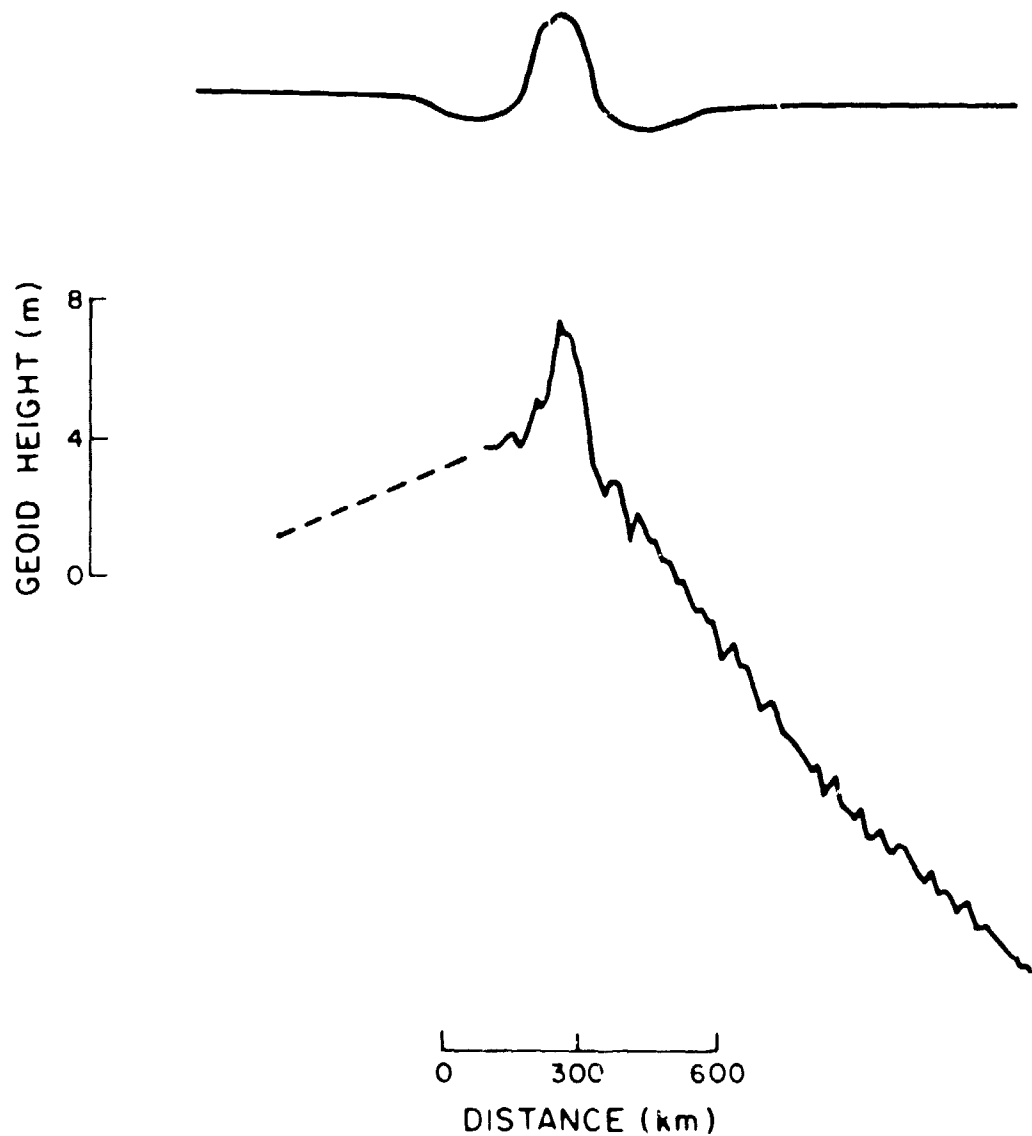


Figure 6. Same as Figure 10 for satellite revolution number 7024

In the central section, we again applied both models. The thin-elastic-plate model gives best fitting theoretical geoid heights for a flexural-rigidity value of the order of 5×10^{29} dyne-cm. Again in this case, there is a discrepancy between the observed and the computed geoid heights for the width and negative aisles of the signal. By using a crustal thickness of 25 km, the Airy model gives a better fit for all parameters than the thin-elastic-plate model does.

The situation is reversed, however, for the western section of the Walvis Ridge. The signal is sharp and narrow and is matched very well by the thin-elastic-plate model when a flexural-rigidity value of about 0.8 to 1.0×10^{29} dyne-cm is used (see Figures 7 and 8). This value would thus suggest that the seamounts were formed on very young and very thin lithosphere, of the order of 8 to 10 km thick. These values for the lithospheric thickness are similar to but larger than those found by Detrick and Watts (1979) in the same area in their correlation of surface ship gravity data and bathymetry data. The slight discrepancy can be easily accounted for by the nature of the bathymetry used in our study. Our bathymetry profiles were reconstructed along the subsatellite positions from the Uchupi bathymetric charts, which have 400-m intervals between contours; thus, we could overestimate the depth of the bottom floor and underestimate the ridge height by as much as 399 m. We performed the calculations a second time using visual interpolation for points between bathymetry contours. This lowered the flexural rigidity to 6×10^{29} dyne-cm, in perfect agreement with other researchers.

We also studied the Rio Grande Rise in the South Atlantic Ocean. This area was chosen in order to be compared with the previously studied Walvis Ridge area, because it is located symmetrically with respect to the Mid-Atlantic Ridge. The geoid signals present in the Rio Grande Rise region are weak and broad and mainly resemble those observed in the eastern and central sections of the Walvis Ridge. At this point in the study, we believe that the Rio Grande Rise has been formed simultaneously with the eastern and central sections of the Walvis Ridge by a hot spot located on the Mid-Atlantic Ridge. Therefore, an Airy-type model of compensation best describes the signal observed.

B. Study of Several Seamount Chains in the Pacific Ocean

According to Morgan (1972), the main chains of islands in the Pacific are the consequence of the Pacific plate moving over three fixed hot spots located respectively.

- 1) At Hawaii, responsible for the Hawaiian-Emperor Seamount chains.

REV. 2191

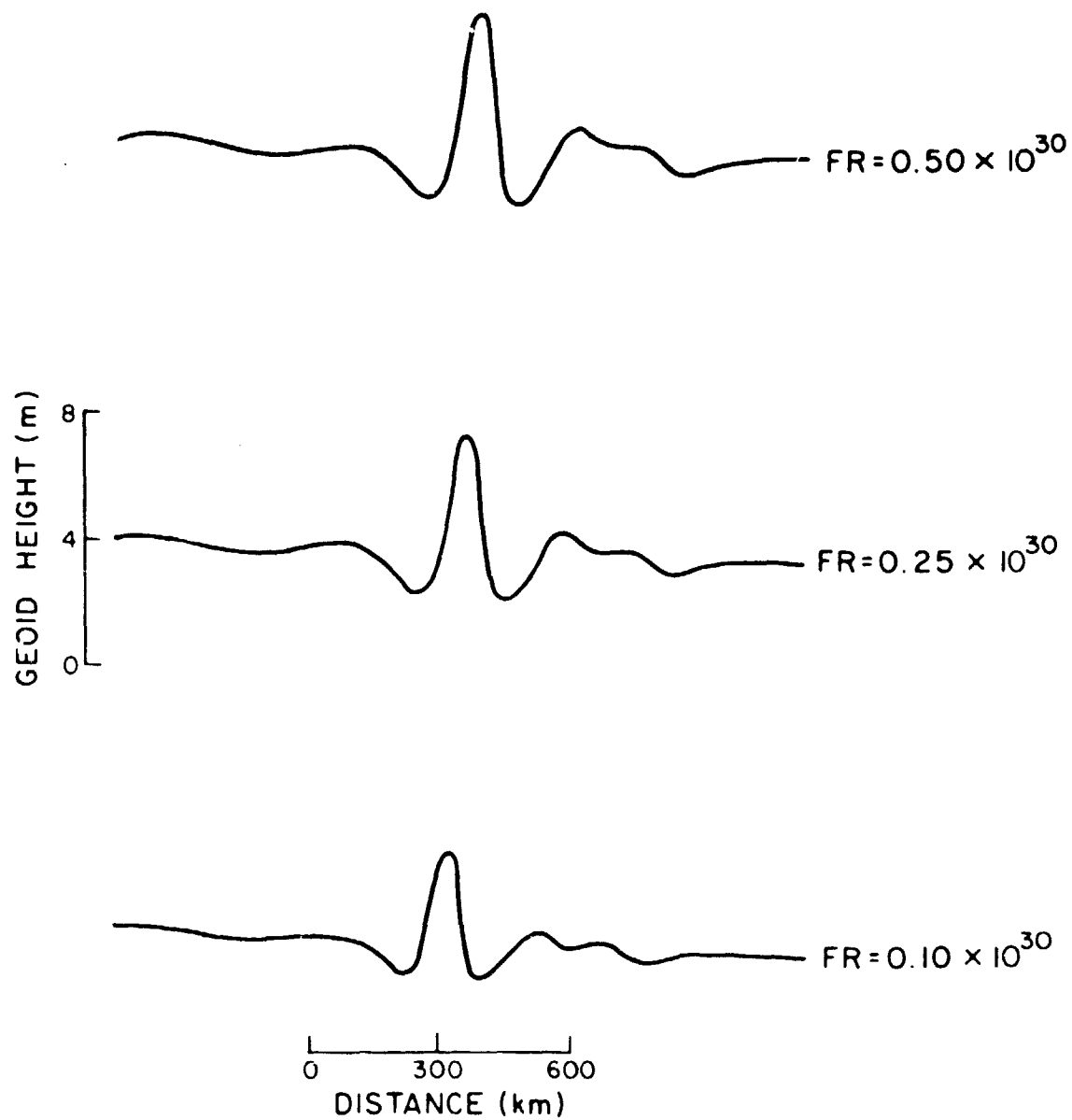


Figure 7. Three predicted geoid heights for satellite revolution number 2191 over Walvis Ridge, calculated from the thin-elastic-plate model with flexural-rigidity values of 0.50 , 0.25 , and 0.10×10^{30} dyne-cm.

REV. 2447

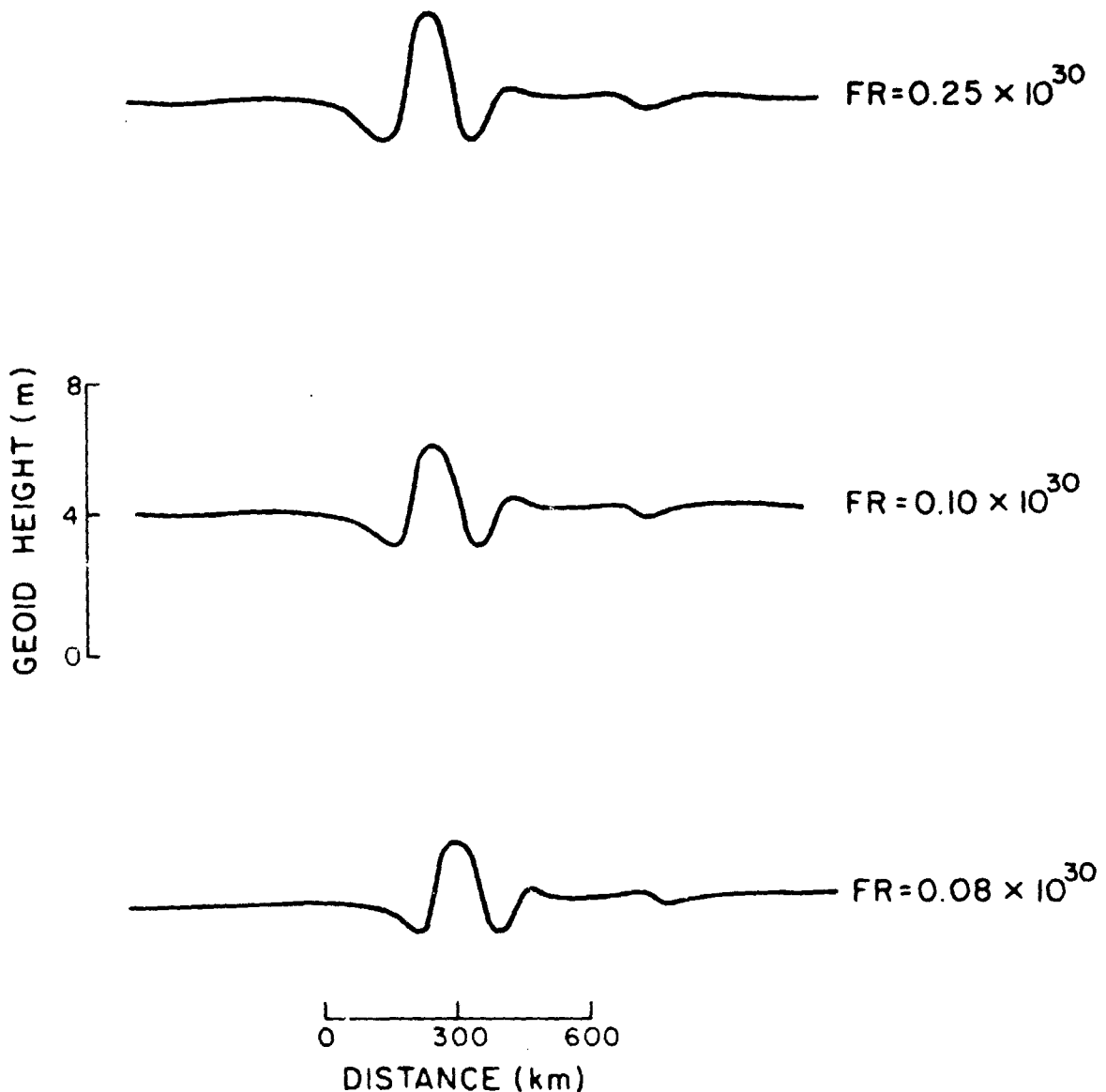


Figure 8. Same as Figure 12 for satellite revolution number 2447 and for flexural-rigidity values of 0.25 , 0.10 , and 0.08×10^{30} dyne-cm.

2) At McDonald, responsible for the Austral, Tubuai, Marshall-Gilbert seamount chains.

3) At the intersection of the East Pacific Rise and the Tuamotu and Sala y Gomez ridges, responsible for the Tuamotu-Line seamount chains. This can be seen in Figure 9. The age of these seamounts thus increases towards the northwest.

The Hawaiian-Emperor Seamount chains have first been studied and the results have been reported in Roufosse (1979). The values for the flexural rigidity range between 1 and 3×10^{30} dyne-cm for the Hawaiian chain and between 5 and 8×10^{29} dyne-cm for the Emperor chain. These results are in agreement with those reported by Watts (1978) using surface ship gravity data.

The next features studied are the chains of seamounts produced by the hot spot located at the intersection of the East Pacific Rise and the Tuamotu and Sala y Gomez ridges: the Tuamotu-Line chains. The Tuamotu Islands constitutes the youngest section of this alignment; their ages range between 37 and 40 M.Y. while the Line island ages range between 40 and 97 M.Y. The lithosphere underlying the Line Seamounts is of the order of 80 to 100 M.Y., whereas that underlying Tuamotu Seamount is younger, of the order of 70 M.Y. The lithosphere was thus older when it was loaded by the Tuamotu Seamounts than by the Line Islands. The values for the flexural rigidity that best predicts the behavior of the geoid for the Line Islands is of the order of 1.0 to 2.5×10^{29} dyne-cm while it ranges between 2.5 and 5.0×10^{29} dyne-cm in the case of the Tuamotu Islands. In Figures 10 and 11 you can see respectively the observed and predicted geoid heights in the case of the Line Islands. Figure 12 represents the observed and predicted geoid heights and the bathymetry of the Tuamotu Islands.

Finally, we have studied the two chains of seamounts produced by the McDonald hot spot. The Tubuai Austral Cook Seamounts are quite young; their ages range between 5 and 25 M.Y. The Marshall-Gilbert Seamounts constitute the oldest section with ages varying between 40 and 70 M.Y. The values for the flexural rigidity associated with the youngest seamounts vary between 7.5×10^{29} and 10^{30} dyne-cm while that associated with Marshall-Gilbert ranges between 2.5 and 5×10^{29} dyne-cm. Figure 13 represents the geoid signals associated with two seamounts of different ages but similar size and loading lithosphere roughly the same age. The left smaller signal is associated with the older seamount (Tuamotu chain) while the right more intense signal is associated with the younger seamount (Tubuai chain). It is quite clear that they cannot be explained and reproduced from bathymetry with the same correlation function. The younger seamount requires a larger value for the flexural rigidity 7.5×10^{29} dyne-cm versus 2.5×10^{29} dyne-cm for the older seamount.

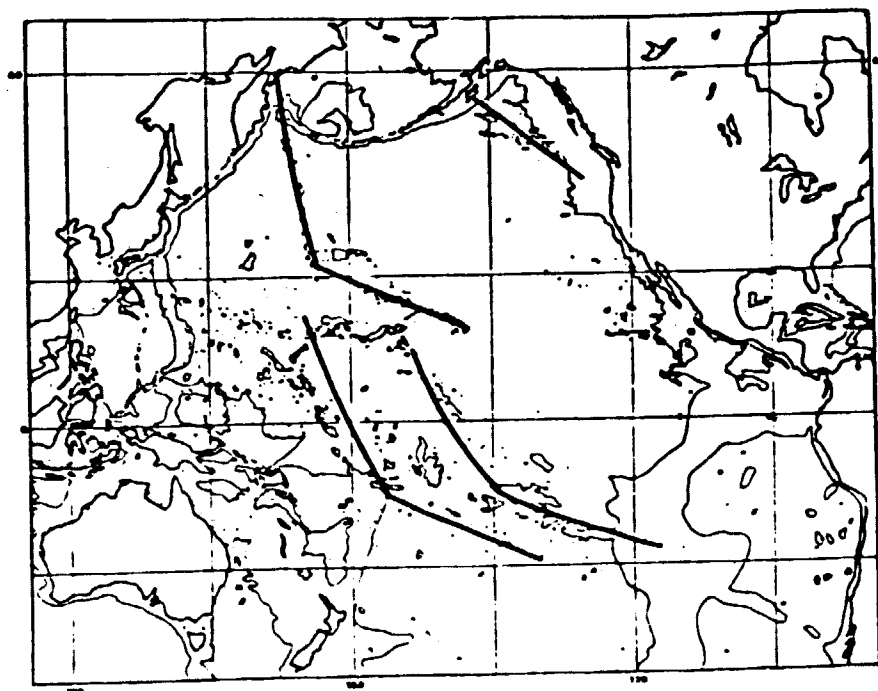


Figure 9. Hot spot trajectories in the Pacific plate.

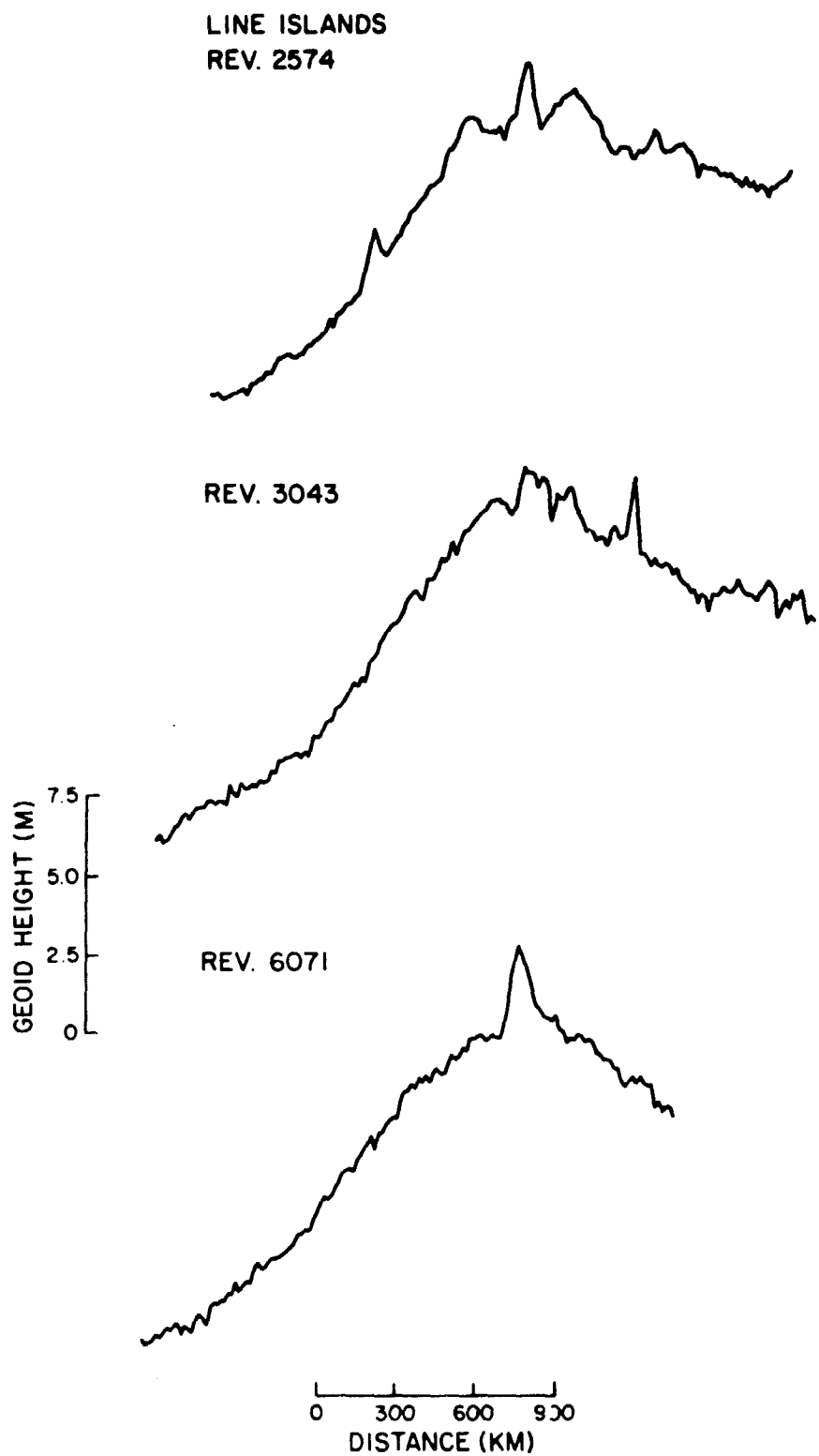
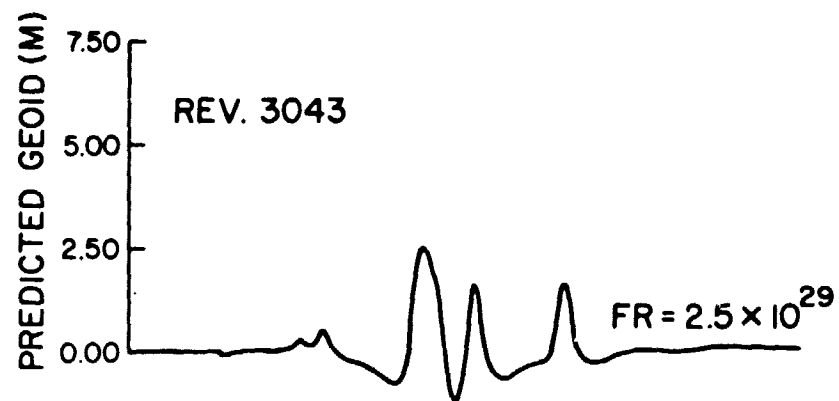


Figure 10. Three geoid height profiles crossing the Line Seamount chain. They are represented with respect to a reference geoid of degree and order calculated with GEM 10.

LINE ISLANDS
REV. 2574



REV. 6071

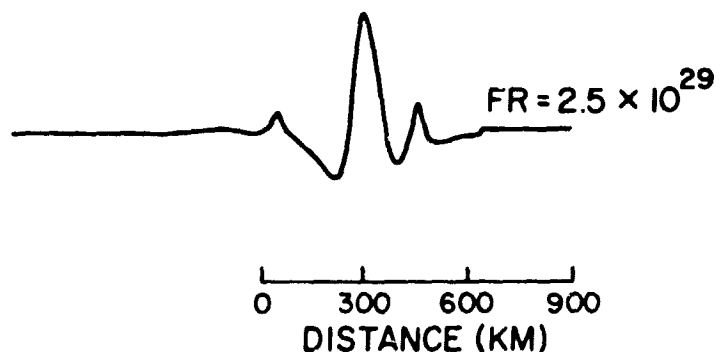


Figure 11. Three predicted geoid height profiles crossing respectively the Line Seamounts chain at the same locations as the observed geoid height profiles shown on Figure 2.

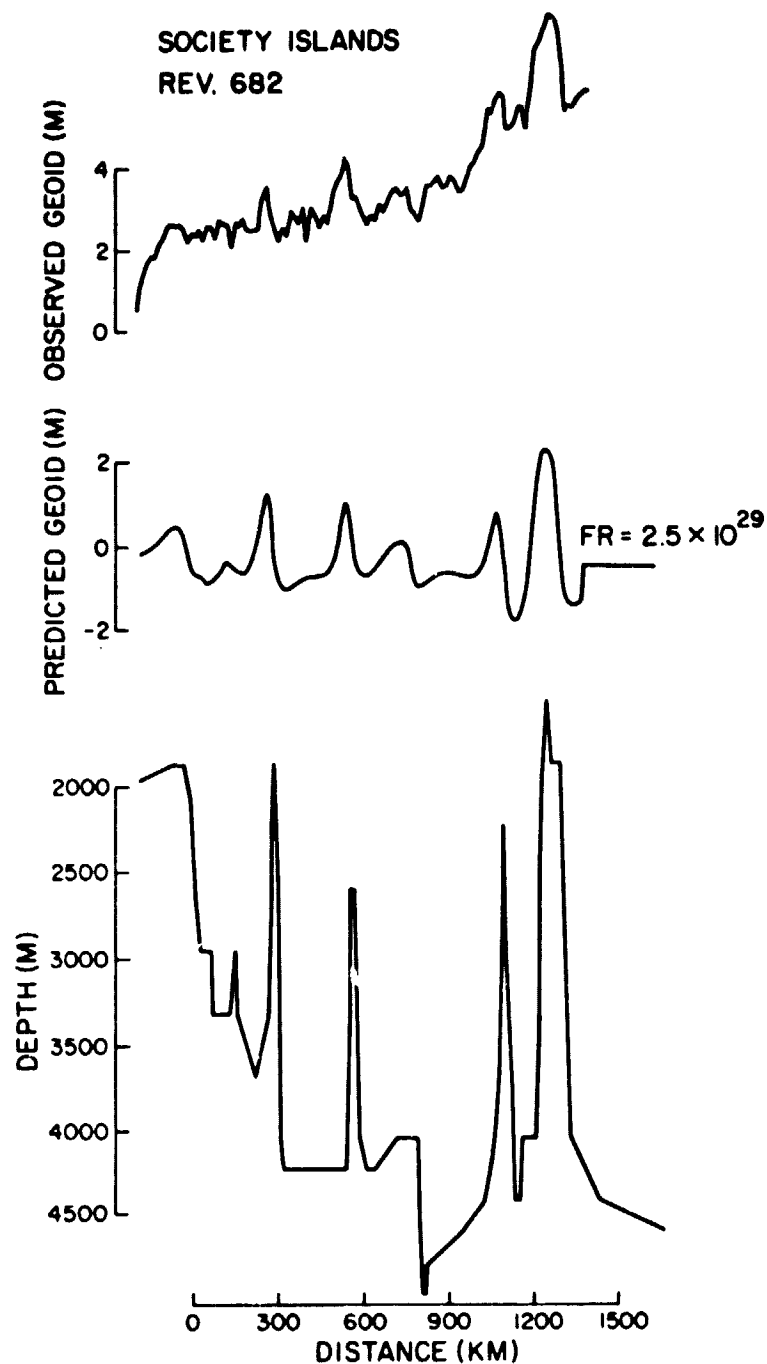


Figure 12. The top profile represents the observed geoid height with respect to a reference geoid of degree and order 16 calculated with GEM 10 across the Tuamotu Seamounts chain. The intermediate profile represents the predicted geoid height profile calculated with a value for the flexural rigidity of 2.5×10^{29} dyne-cm. The bottom profile represents the bathymetry reconstructed from contour charts along the subsatellite positions.

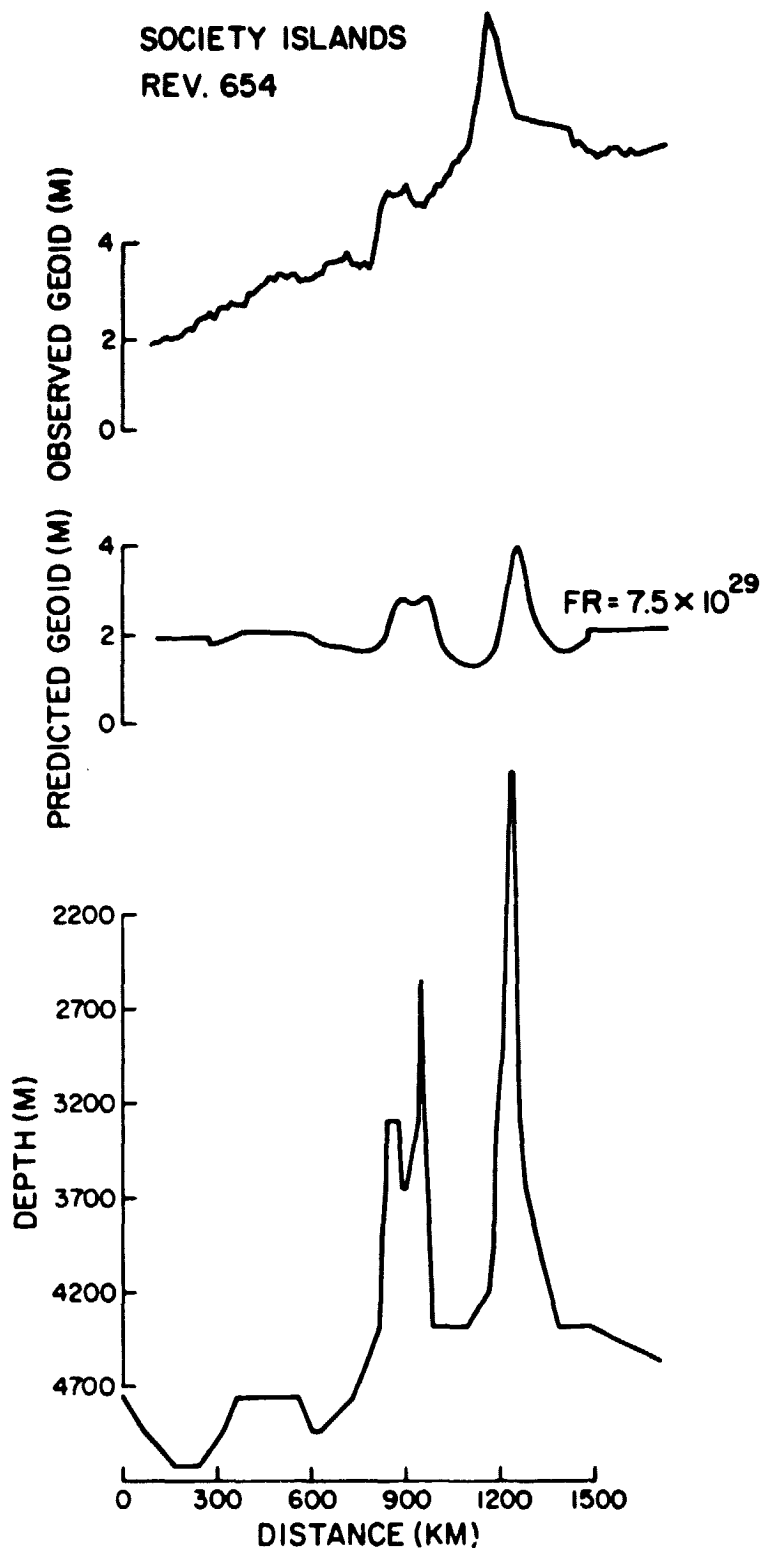


Figure 13. Same as Figure 4 for a profile crossing the Marshall Seamounts chain.

The parameter which mostly influences the geoid signal is thus the age of the lithosphere at the time of loading. Quantitatively, the agreement is quite reasonable, taking into account the large uncertainties in the prediction of the ages of the seamounts; from the values for the flexural rigidity, we calculated that the lithosphere was roughly twice as old when it was loaded by Tubuai than by Tuamotu, in good agreement with available age data.

C. Study of the North Atlantic Ocean

1) New England Seamounts

Two typical passes over the New England seamounts can be seen on the top profiles of Figures 14 and 15. The signals observed have a wavelength of 150 to 200 km and an intensity of 2 to 4 m. It is similar to the signal observed in the Marshall-Gilbert seamounts area; all the values found for the flexural rigidity are very low. These values range between 1×10^{29} and 4×10^{29} dyne-cm. The lithosphere is known to be very old in this region and therefore it is very strong. In order to account for the low values of the flexural rigidity, we had to postulate that the seamounts were very old and, therefore, were formed when the lithosphere was younger and thinner. The information gathered on the age of the seamounts confirms that hypothesis.

2) North Atlantic Ridge and Azores

Now, we are in the process of retrieving several passes over the northern Mid-Atlantic Ridge and over the Azores Islands in order to study both the short and intermediate wavelengths that are present in the geoid spectrum.

Twenty-nine SEASAT passes and sixty GEOS-3 passes have been retrieved in that area. The GEOS-3 data are being filtered for long wavelengths (a reference geoid of degree and order 10 calculated with GEM 7 is removed from the raw data), and corrected for bias and trend using Dr. Rapp's information. It will then be plotted on Mercator projection in a collaborative effort with Dr. Parsons (MIT) and Dr. McKenzie (Cambridge University, U. K.).* This map will give information on the intermediate wavelengths contained in the geoid and will be suitable for a time dependence study. The SEASAT data are studied on a track-by-track basis, and attention is focussed on the small wavelength features. We are presently in the process of retrieving the bathymetry along individual passes.+

*Effort supported by Smithsonian Scholarly Studies program Grant 1240S102-P12G00-4G50 and proposed under SAO Proposal P-1001-7-80.

+Continuing effort supported by NASA Grant NAG5-150 beginning 1 March 1981.

REV. 529

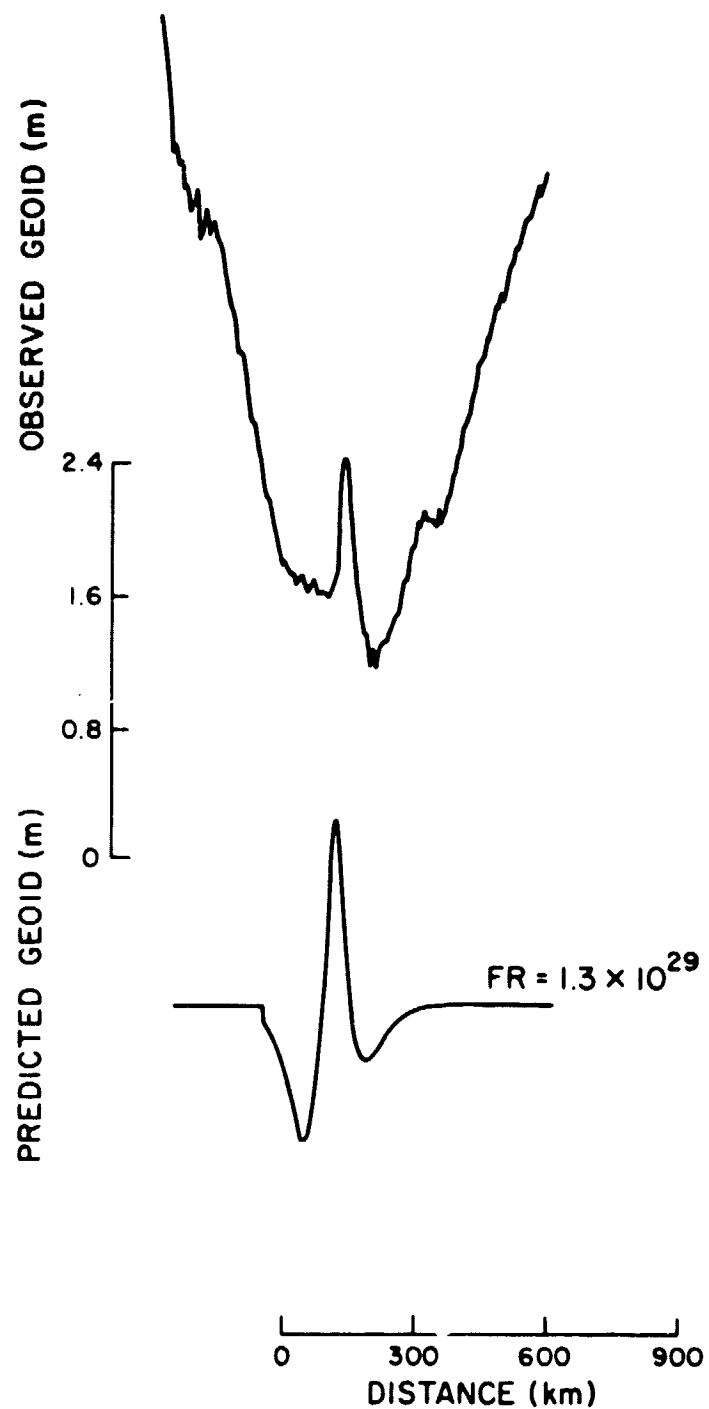


Figure 14. The top profile represents the observed geoid heights for the Seasat revolution number 529 over the New England seamounts. The bottom profile represents the predicted geoid heights calculated with a value for the flexural rigidity of 1.3×10^{29} dyne-cm.

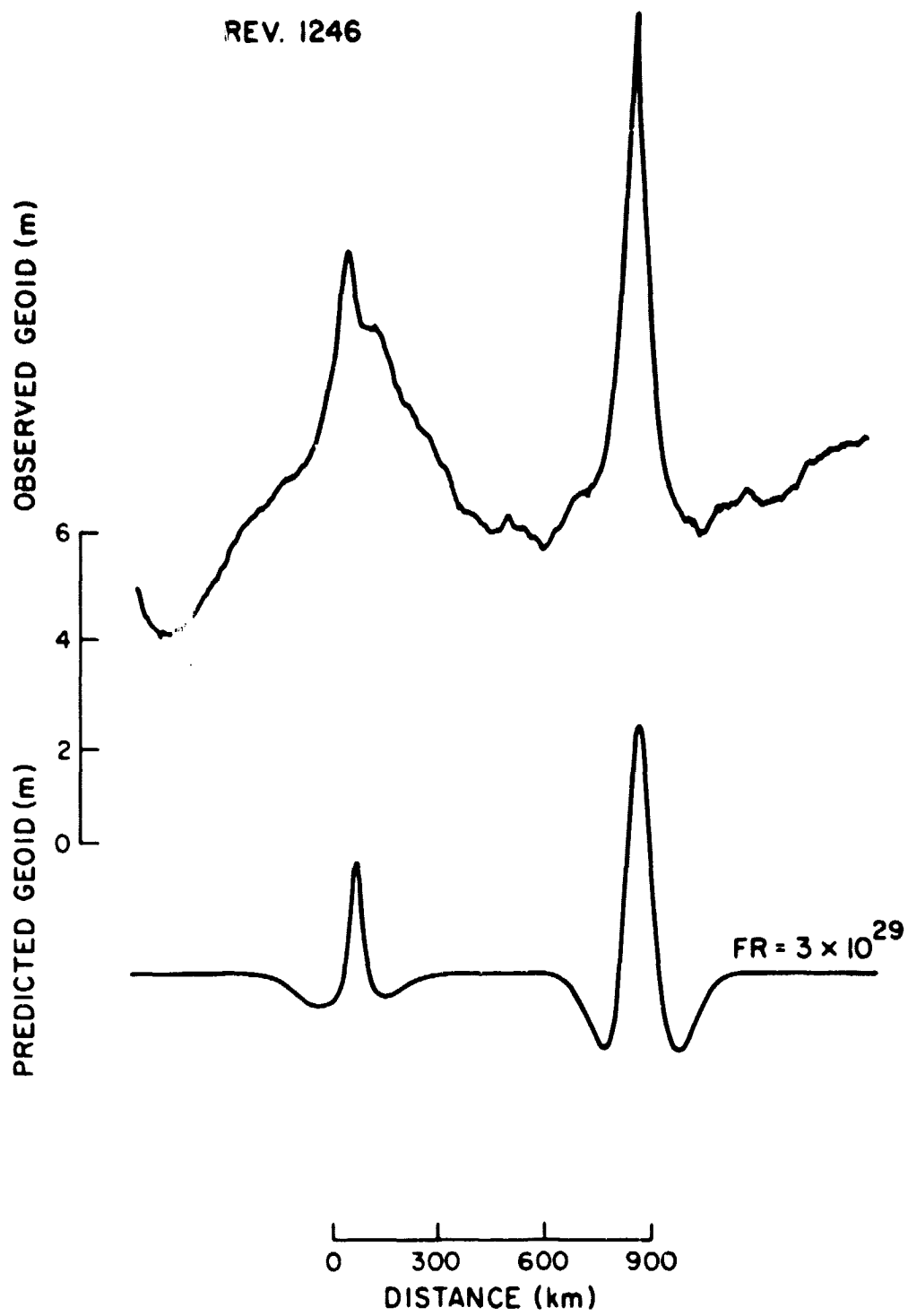


Figure 15. The top profile represents the observed residual geoid heights for the Seasat revolution number 1246 over the New England seamounts. The bottom profile represents the predicted geoid heights calculated with a value for the flexural rigidity of 3×10^{29} dyne-cm.

IV Conclusions

So far, we have studied a large variety of bathymetric features spanning different lithospheric ages and conditions of creation and evolution. The two main factors that seem to influence the geoid heights are the conditions of creation (e. g., hot spot and uplift) on the one hand and the age of the lithosphere at the time of loading (e. g., position with respect to the ridge axis) on the other hand. The latter point requires further investigation, however, because it seems that the actual lithospheric age should be present in the geoid signal. In future research, we hope to resolve that discrepancy by using both GEOS-3 and SEASAT radar altimeter data acquired over several other bathymetric features*.

*See footnotes, page 20.

References

Detrick, R. S., and Watts, A. B., 1979. An analysis of isostasy in the world's oceans: Part 3 - Aseismic ridges. *Journ. Geophys. Res.*, Vol. 84, pp. 3637-3653.

Dingle, R. V., and Simpson, E. S. W., 1976. The Walvis Ridge: A review. In Geodynamical Progress and Prospects, ed. by C. L. Drake, American Geophysical Union, Washington, D. C., pp. 160-176.

Ewing, M., Le Pichon, X., and Ewing, J., 1966. Crustal structure of the mid-ocean ridges: 4-sediment distribution in the south Atlantic Ocean and the Cenozoic history of the Mid-Atlantic Ridge. *Journ. Geophys. Res.*, vol. 71, pp. 1611-1635.

Francheteau, J., and Le Pichon, X., 1972. Marginal fracture zone as structural framework of continental margins in the South Atlantic Ocean. *Amer. Assoc. Petroleum Geol. Bull.*, vol. 56, pp. 991-1007.

Goslin, J., Mascle, J., Sibuet, J. C., and Hoskins, H., 1974. Geophysical study of the easternmost Walvis Ridge, South Atlantic: Morphology and shallow structure. *Geol. Soc. Amer. Bull.*, vol. 85, pp. 619-632.

Goslin, J., and Sibuet, J. C., 1975. Geophysical study of the easternmost Walvis Ridge, South Atlantic: Deep structure. *Geol. Soc. Amer. Bull.*, vol. 86, pp. 1713-1724.

Le Pichon, X., and Hayes, D. E., 1971. Marginal offsets, fracture zones and the early opening of the South Atlantic. *Journ. Geophys. Res.*, vol. 76, pp. 6283-6296.

Maxwell, A. E., Von Herzen, P. P., Hsü, K. J., Andrews, J. E., Saito, T., Percival, S. F., Milow, E. D., Jr., and Boyce, R. E., 1970. Deep sea drilling in the South Atlantic. *Science*, vol. 168, pp. 1047-1059.

McKenzie, D. P., and Bowin, C., 1976. The relationship between bathymetry and gravity in the Atlantic Ocean. *Journ. Geophys. Res.*, vol. 81, pp. 1903-1915.

Morgan, W. J., 1971. Convection plumes in the lower mantle. *Nature*, vol. 230, pp. 42-43.

Morgan, W. J., 1972a. Deep mantle convection plumes and plate motions. *Amer. Assoc. Petroleum Geol. Bull.*, vol. 56, pp. 203-213.

Morgan, W. J., 1972b. Plate motions and deep mantle convection. *Geol. Soc. Amer. Mem.*, vol. 132, pp. 7-22.

Roufosse, M., 1979. Interpretation of altimeter data. In An International Symposium on the Applications of Geodesy to Geodynamics, Proceedings of the 9th GEOP Conference, Ohio State Univ., Dept. Geod. Sci., Rep. No. 280, pp. 261-266.

Watts, A. B., 1978. An analysis of isostasy in the world's oceans, Hawaiian-Emperor Seamount chain. *Journ. Geophys. Res.*, vol. 83, pp. 5989-6004.